The Journal of Chemical Physics

UV emission of I_2 from the ion-pair state following amplified spontaneous emission

Cite as: J. Chem. Phys. **128**, 164320 (2008); https://doi.org/10.1063/1.2898881
Submitted: 31 October 2007 . Accepted: 26 February 2008 . Published Online: 30 April 2008

Yukio Nakano, Hisashi Fujiwara, Masaru Fukushima, and Takashi Ishiwata

AIP Publishing

UV emission of I_2 from the ion-pair state following amplified spontaneous emission

Yukio Nakano, Hisashi Fujiwara, Masaru Fukushima, and Takashi Ishiwata[a)]
Graduate School of Information Sciences, Hiroshima City University, Ozukahigashi, Asaminami, Hiroshima 731-3194, Japan

(Received 31 October 2007; accepted 26 February 2008; published online 30 April 2008)

This paper reports the results of processes resulting in $D0_u^+$-$X\ ^1\Sigma_g^+$ emission when a single rovibrational level of the $E0_g^+$ state is prepared. Our study reveals that two kinds of processes populate the $D0_u^+$ state; which one occurs depends on the experimental conditions. One process involves amplified spontaneous emission from the $E0_g^+$ state. The other is collision-induced energy transfer in self-quenching. We distinguish these two processes from the time profiles of fluorescence signals. These processes give completely different vibrational distributions in the $D0_u^+$ state from a given rovibrational level of the $E0_g^+$ state. The discrepancy between our results and previous results for the $E0_g^+ \rightarrow D0_u^+$ relaxation is briefly discussed. © *2008 American Institute of Physics*. [DOI: 10.1063/1.2898881]

I. INTRODUCTION

Molecular iodine has a series of excited states that are correlated with the atomic ions $I^-(^1S)+I^+(^3P, ^1D, \text{and } ^1S)$ at the dissociation limit.[1] Enormous effort has been made to understand their electronic structures in conjunction with the development of laser excitation techniques, and a great volume of spectroscopic data exists in the literature.[2–5] Under this situation, there has been renewed interest in these excited states due to the possibility that could be used to provide a benchmark for studies on inelastic collisions of electronic energy transfer.

The lowest dissociation limit of $I^-(^1S)+I^+(^3P_2)$ gives six ion-pair states lying ~41 000 cm^{-1} above the $X\ ^1\Sigma_g^+$ ground state. They are usually designated, in the order of increasing energy, as $D'2_g$, $\beta 1_g$, $D0_u^+$, $E0_g^+$, $\gamma 1_u$, and $\delta 2_u$ using the traditional labeling and Hund's case (c) notation. The ion-pair states have strongly bonded potential curves, which are characterized by very similar, but not exactly equal, equilibrium distances and spectroscopic constants. Recent studies established excitation schemes for attaining these states for various symmetries by using optical-optical double resonance.[6–10] This technique facilitates the study of the efficiency and selectivity of energy transfer between these states, in terms of symmetries, Franck–Condon factors, energy matching, etc., by collecting emissions to the lower lying valence states. One of the problems that has arisen from these results is the marked difference in the energy transfer rate constants reported for the $E0_g^+ \rightarrow D0_u^+$ collision-induced nonadiabatic transition.

The $E0_g^+ \rightarrow D0_u^+$ relaxation process in collision with $I_2(X)$ was first analyzed by Ubachs *et al.*[11] from a spectroscopic viewpoint. From the $D0_u^+$-$X\ ^1\Sigma_g^+$ fluorescence observed after excitation to the $E0_g^+$ $v=8$ state, the $D0_u^+$ state was found to have quite a narrow population distribution, principally governed by vibrational energy transfer to $I_2(X)$. Teule *et al.*[12] in the same group extended the initial excitation of the $E0_g^+$ state to $v_E=8-23$. With this increase in the vibrational energy of the $E0_g^+$ state, the vibrational distribution of the $D0_u^+$ state changed to that governed by the minimum energy transfer, similar to those found in collisions with Ar, N_2, and O_2. On the other hand, for the excitation of $v_E=1$, Inard *et al.*[13] found the strong rotational propensity rule $\Delta J=\pm 1$ in the $E0_g^+ \rightarrow D0_u^+$ relaxation and the vibrational propensity governed by the vibrational excitation of the $X\ ^1\Sigma_g^+$ state, similar to that found for the $v_E=8$ state.

The rate constant of the $E0_g^+ \rightarrow D0_u^+$ collision-induced energy transfer by $I_2(X)$ was measured by Akopyan *et al.*[14] at the excitation of $v_E=47-58$. This experiment was recently extended to the lower vibrational states $v_E=8-23$ by Bibinov *et al.*[15] in the same group. The total rate constants were found to vary between 7×10^{-10} and 80×10^{-10} cm^3 $molecule^{-1}$ s^{-1} and exhibited sharp maxima as a function of v_E, as summarized in their recent review.[16] The hard-sphere collision cross section at the maxima reached the huge value of 3300 $Å^2$, which is approximately 40 times larger than the gas-kinetic cross section. An "approach-induced" model was then proposed to interpret the large cross section for collision partners with permanent or transition electrostatic moments under the quasi-resonant condition, i.e., that the energy gap between the initial and final states does not exceed 25 cm^{-1}. On the other hand, Fecko *et al.*[17] reported the corresponding rate constant at $v_E=0$ as $k=4.0\times10^{-11}$ cm^3 $molecule^{-1}$ s^{-1}, which is an order of magnitude smaller than the extrapolated value from the approach-induced model.[16] At the same time, with an increase in the I_2 pressure, they observed the occurrence of an extraordinary strong $D0_u^+$-$X\ ^1\Sigma_g^+$ emission whose vibrational distribution was very different from that observed in collision-induced relaxation, but the generation mechanism of strong $D0_u^+$-$X\ ^1\Sigma_g^+$ emission was unsettled. Recently, Alekseev *et al.*[18] reported evidence for amplified spontaneous

[a)]Author to whom correspondence should be addressed. Electronic mail: ishiwata@im.hiroshima-cu.ac.jp.

emission (ASE) between the $E0_g^+$ and $D0_u^+$ states when the $E0_g^+$ state is populated by optical-optical double resonance. They attributed it to the process for sufficiently populating the $D0_u^+$ state to enable the strong $D0_u^+$-$X\ ^1\Sigma_g^+$ emission observed by Fecko *et al.*[17] Ridley *et al.*[19] in the same group used this effect to populate the $D0_u^+$ state and analyzed the shallow 0_g^+ state correlating to $I(^2P_{1/2})+I(^2P_{1/2})$ from the dispersed emission spectra.

Recently, we commenced a program of study with the aim of understanding the radiative and collisional relaxation of the $E0_g^+$ state and to resolve the problems encountered in interpreting earlier experimental results. The first problem to be addressed concerns the processes that give rise to the $D0_u^+$-$X\ ^1\Sigma_g^+$ emission when a single rovibrational level of the $E0_g^+$ state is prepared. Our study reveals that two kinds of processes populate the $D0_u^+$ state. Which one occurs depends on the experimental conditions. One is the process involving amplified spontaneous emission from the $E0_g^+$ state, which was proposed by Alekseev *et al.*[18] The other is collision-induced energy transfer in self-quenching, which was studied by Fecko *et al.*[17] We distinguish these two processes from the time profiles of fluorescence signals. These processes give completely different vibrational distributions in the $D0_u^+$ state from a given rovibrational level of the $E0_g^+$ state. Furthermore, the time profiles of fluorescence signals denote the self-quenching rate constant of $(8.8\pm0.7)\times10^{-10}$ cm^3 molecules^{-1} s^{-1} in the $E0_g^+$ $v=0$ state, which is more than an order of magnitude larger than that observed for the collision-induced energy transfer that gives the $D0_u^+$ state.

II. EXPERIMENTAL

The experiments were performed in a pump and probe system, which was described in a previous publication by Nakano *et al.*[4] Briefly, two dye lasers were pumped by the divided outputs of a Q-switched Nd^{3+} doped yttrium aluminum garnet laser and they were used as excitation sources to prepare I_2 in a single rovibrational level of the $E0_g^+$ state. One dye laser was operated at ~550 nm to excite the $B\ ^3\Pi(0_u^+)$-$X\ ^1\Sigma_g^+$ transition. After a suitable delay, the other dye laser excited a fraction of the $B\ ^3\Pi(0_u^+)$ state population to the $E0_g^+$ state using the $E0_g^+$-$B\ ^3\Pi(0_u^+)$ transition at ~425 nm. Each laser pulse had a 7 ns temporal width and a spectral resolution of 0.2 cm^{-1}. The time delay between two laser pulses was adjusted to be 20 ns using an optical delay line, so as to prevent temporal overlap of pump and probe laser pulses. The I_2 cell was a quartz tube with parallel windows and a side window at the center of cell. The length of the cell was typically 10 cm. The beam diameter of the pump laser was expanded to 5 mm using a telescope, and that of the probe laser was typically 3 mm.

Double resonance excitation of I_2 resulted in intense $E0_g^+$-$B\ ^3\Pi(0_u^+)$ emission with some associated band systems. The emission spectra were observed through a 30 cm monochromator (MS257, Oriel Instruments) equipped with a 2400 grooves/mm grating. Two spatial arrangements of the pump and probe lasers beams were used to excite I_2. In one, the two laser beams passed through the sample cell by intersecting at angle of 30° in front of the monochromator slit. In the other, the beams were coaxially collimated along the slit. In each case, the emissions were detected through the side window in the direction perpendicular to the laser beams. The ASE measurements were performed by detecting the backward emission along the axis of the coaxially aligned laser beams. The signals from a photomultiplier were processed by a boxcar and stored on a personal computer.

After passing through the monochromator, the transient signals of ultraviolet emission were detected using a fast photomultiplier tube with a rise time of 0.8 ns. The photomultiplier signals were stored and averaged using a digital oscilloscope to eliminate the shot-to-shot variation of fluorescence intensities.

III. RESULTS AND DISCUSSION

A. Excitation to the $E0_g^+$ ion-pair state

Following the optical selection rules for single-photon transitions, the $E0_g^+$ ion-pair state is accessible from the $X\ ^1\Sigma_g^+$ ground state in the (1+1) photoexcitation sequence,

$$E0_g^+ \overset{h\nu_2}{\leftarrow} B\ ^3\Pi(0_u^+) \overset{h\nu_1}{\leftarrow} X\ ^1\Sigma_g^+.$$

In this stepwise process, the intermediate $B\ ^3\Pi(0_u^+)$ state compromises the large Franck–Condon shift required for the transition between the $E0_g^+$ and $X\ ^1\Sigma_g^+$ states. Since the excitation efficiency is dominated by the Franck–Condon factors of two transition components, we selected and used the $v=20-32$ vibrational levels of the $B\ ^3\Pi(0_u^+)$ state to access the lower vibrational levels of the $E0_g^+$ state. The excitation to the $E0_g^+$ state was easily identified by the strong emission radiating back to the $B\ ^3\Pi(0_u^+)$ state at around 425 nm. The excitation schemes were then assigned from the pump and probe laser frequencies by referring to a spectral atlas calculated from the known spectroscopic constants of the electronic states involved in the transitions.

Apart from the $E0_g^+$-$B\ ^3\Pi(0_u^+)$ emission, three emission systems have been observed with appreciable intensities in the 300–350 nm range (for example, see Fig. 2 in Ref. 17). One is the broad band system at ~347 nm, which is assigned to the $E0_g^+$-$B''\ ^1\Pi_u(1_u)$ transition. Another is the discrete band at ~335 nm assigned to the $E0_g^+$-$A\ ^3\Pi(1_u)$ transition. They have the upper state in common with the $E0_g^+$-$B\ ^3\Pi(0_u^+)$ transition. Due to the $\Delta\Omega=0$ propensity rule for the charge-transfer transitions, the intensities of these two perpendicular $\Delta\Omega=\pm1$ transitions were about by two orders of magnitude weaker than that of the $E0_g^+$-$B\ ^3\Pi(0_u^+)$ transition. The other is the discrete emission lying in the range of 300–330 nm, which is attributed to the $D0_u^+$-$X\ ^1\Sigma_g^+$ transition under study. Two emission spectra exhibiting different vibrational distributions were found to occur in this system depending on the experimental conditions.

Figure 1 shows examples of the $D0_u^+$-$X\ ^1\Sigma_g^+$ emission observed at the excitation to the $E0_g^+$ $v=0$ and $J=55$ state. They were recorded at an I_2 pressure of 0.173 Torr. The output of the dye laser was 1 mJ/pulse for the pump laser and 0.3 mJ/pulse for the probe laser. Spectrum (a) has features indicating broader vibrational distribution in the $D0_u^+$ state.

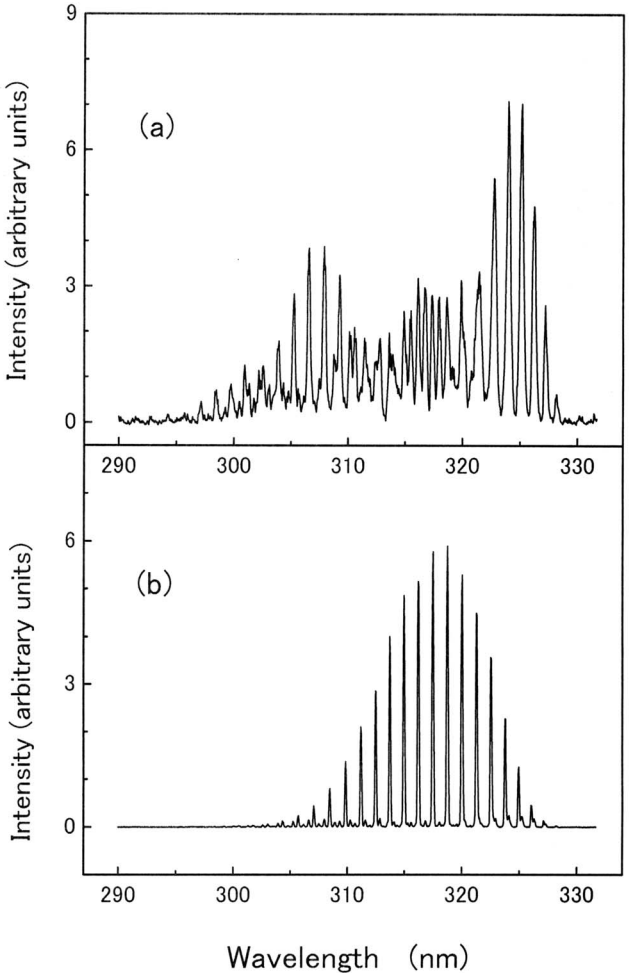

FIG. 1. The two types of emission spectra that were observed from the $D0_u^+$ state, when the $E0_g^+$ $v=0$ and $J=55$ state was populated by the excitation scheme

$$E0_g^+ \overset{(0\text{–}20)\mathrm{P56}}{\underset{h\nu_2}{\leftarrow}} B\,^3\Pi(0_u^+) \overset{(20\text{–}0)\mathrm{R55}}{\underset{h\nu_1}{\leftarrow}} X\,^1\Sigma_g^+,$$

where $h\nu_1=17\,858.7$ cm^{-1} and $h\nu_2=23\,442.9$ cm^{-1}. Spectrum (a) was recorded by intersecting the pump and probe laser beams at an angle of 30° in front of the monochromator slit in exciting I_2. The emission was viewed perpendicular to the plane of the laser beams. On the other hand, spectrum (b) was recorded by coaxially aligning the pump and probe laser and by passing the laser beams along the monochromator slit. The output of the dye laser is 1 mJ/pulse for the pump laser beam and 0.3 mJ/pulse for the probe laser beam. The spectral slit width of the monochromator was 0.30 nm for spectrum (a) and 0.15 nm for spectrum (b). The I_2 sample pressure was 0.173 Torr.

The integrated emission intensity is about half of those observed in the perpendicular transitions from the $E0_g^+$ state. To obtain this spectrum, we intersected two laser pulses at an angle of approximately 30° in front of the monochromator slit and tried to minimize the length of the overlap region between the two laser beams. On the other hand, spectrum (b) has a simple structure, which is attributed to the emission mostly from the $D0_u^+$ $v=0$ state. It was recorded by coaxially aligning two laser beams and overlapping them in front of the monochromator slit without changing the other conditions that were used to take spectrum (a), including the excitation scheme, laser power, and time delay between laser pulses. The $D0_u^+$-$X\,^1\Sigma_g^+$ emission in spectrum (b) is dramatically more intense than in spectrum (a), and its intensity is similar to that of the $E0_g^+$-$B\,^3\Pi(0_u^+)$ emission. This increase of the emission intensity by two orders of magnitude cannot be attributed to the influence of the effective volume in exciting I_2. The different vibrational distributions between spectra (a) and (b) indicate that the $D0_u^+$ state was populated by different mechanisms through the $E0_g^+$ state in these spectra.

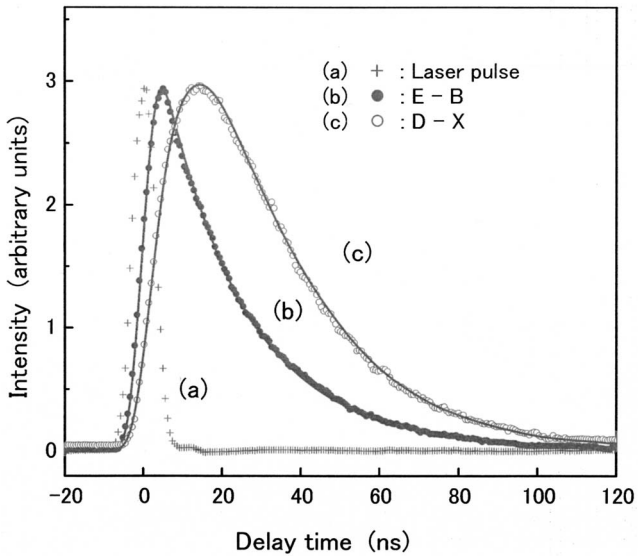

FIG. 2. The time profiles of emission intensities observed in the $E0_g^+$-$B\,^3\Pi(0_u^+)$ and $D0_u^+$-$X\,^1\Sigma_g^+$ system, showing the $D0_u^+$ state populated by collision-induced energy transfer from the $E0_g^+$ state. Waveform (a) is the profile of the probe laser pulse. Waveform (b) was detected at 424.6 nm using the (0–19) band of the $E0_g^+$-$B\,^3\Pi(0_u^+)$ system with a spectral slit width of 0.15 nm. Waveform (c) was detected at 325.0 nm for the $D0_u^+$-$X\,^1\Sigma_g^+$ system with a spectral slit width of 0.5 nm. In obtaining waveforms (b) and (c), the pump and probe laser beams were intersected at an angle of 30° in front of the monochromator slit and the emission was viewed perpendicular to the plane of the laser beams. The I_2 sample pressure was 0.173 Torr.

Fecko *et al.*[17] reported a spectrum similar to spectrum (a) at 40 mTorr of I_2 using the same technique. They ascribed it to the emission from the $D0_u^+$ state arising from the $E0_g^+$ state by the energy transfer in collision with $I_2(X)$. Furthermore, when the I_2 pressure is increased from 40 to 160 mTorr, the $D\rightarrow X/E\rightarrow A$ integrated intensity ratio increased 75-fold with a fourfold increase in pressure. At the same time, the spectrum features change to that shown in spectrum (b). They proposed a mechanism in terms of the collision-induced processes to explain these spectral changes. However, we found that the spectral features and intensities depend only on the spatial arrangement of the two laser pulses in exciting I_2, and not on the I_2 sample pressure, which obviously conflicts with the collision-induced mechanism. Recently, Alekseev *et al.*[18] suggested that spectrum (b) is caused by $E0_g^+\rightarrow D0_u^+$ radiative relaxation by ASE and not by a collision-induced mechanism. We can distinguish the processes responsible for spectra (a) and (b) by using the time profiles of the emission intensities by employing shorter laser pulses and a fast-response photomultiplier, as described below.

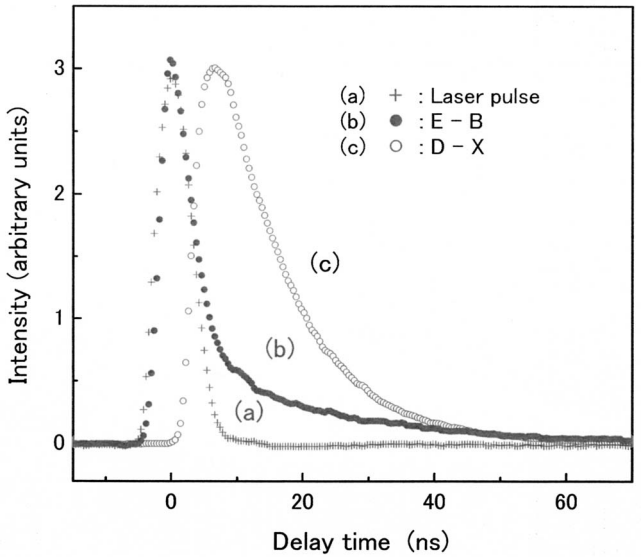

FIG. 3. The time profiles of emission intensities observed in the $E0_g^+$-$B\ ^3\Pi(0_u^+)$ and $D0_u^+$-$X\ ^1\Sigma_g^+$ system, showing the $D0_u^+$ state populated by ASE from the $E0_g^+$ state. Waveform (a) is the profile of the probe laser pulse. Waveform (b) was detected at 424.6 nm using the (0–19) band of the $E0_g^+$-$B\ ^3\Pi(0_u^+)$ system with a spectral slit width of 0.15 nm. Waveform (c) was detected at 318.5 nm using the (0–55) band of the $D0_u^+$-$X\ ^1\Sigma_g^+$ system with a spectral slit width of 0.15 nm. In recording waveforms (b) and (c), the pump and probe laser beams were coaxially aligned. The I_2 sample pressure was 0.173 Torr.

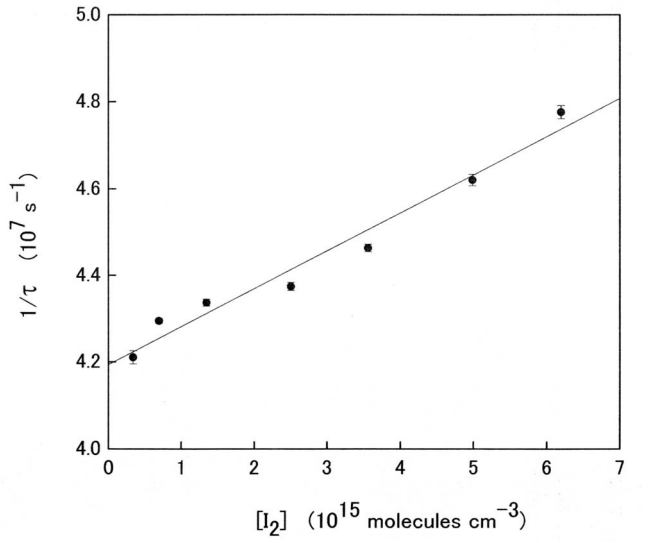

FIG. 4. Stern–Volmer plot for the fluorescence lifetimes of the $E0_g^+$ $v=0$ state against the I_2 concentrations.

B. Time profiles of the emission intensities

Figures 2 and 3 show the time profiles of emission intensities observed in the $E0_g^+$-$B\ ^3\Pi(0_u^+)$ and $D0_u^+$-$X\ ^1\Sigma_g^+$ transitions under the same conditions that we recorded, spectra (a) and (b) shown in Fig. 1, respectively. In these figures, the delay time of $t=0$ is defined as when the probe laser intensity is a maximum.

Figure 2 shows the results, which were recorded by intersecting the pump and probe laser beams by 30° to minimize the length of the overlapping region. Waveform (b) observed for the $E0_g^+$ state was interpreted by the kinetic model on the basis of two processes following the excitation of I_2 to the $E0_g^+$ state:

$$I_2(B) + h\nu \rightarrow I_2(E), \qquad k_{ex}, \tag{1}$$

$$I_2(E) \rightarrow I_2(A,B,B'',D,\text{etc.}) + h\nu, \quad k_r^E, \tag{2}$$

$$I_2(E) + I_2(X) \rightarrow \text{products}, \qquad k_q^E. \tag{3}$$

The rate equations describing these processes indicate that the fluorescence decay curve of the $E0_g^+$ state can be obtained by convoluting a time profile of the probe laser with a single exponential decay.

$$F(t) = C\int^t P(t')\exp[(t'-t)/\tau]dt', \tag{4}$$

where $F(t)$ is the observed fluorescence decay profile and $P(t')$ is the time profile of the probe laser pulse. The value of τ is the fluorescence lifetime defined by

$$1/\tau = k_r^E + k_q^E[I_2], \tag{5}$$

and C is a pre-exponential factor used to adjust the intensity. We adjusted τ and C so as to minimize the standard deviation between the signal and simulation and obtained $\tau = 20.9 \pm 0.1$ ns at 0.174 Torr. Figure 4 shows the variation of fluorescence lifetimes as function of the I_2 concentrations. The resulting value for k_q^E averaged over all pressure is $(8.8 \pm 0.8) \times 10^{-10}$ cm^3 molecules^{-1} s^{-1}. The fluorescence lifetime of the $E0_g^+$ state extrapolated at zero pressure τ_E^0 is 23.9 ± 0.1 ns.

On the other hand, waveform (c) observed for the $D0_u^+$ state can be fitted by convoluting the time profile of the E-B emission [waveform (b)], with a single exponential decay using Eq. (4). It is interpreted by adding reactions (6)–(8) to the kinetic model expressed in reactions (1)–(3), assuming that the $D0_u^+$ state was populated by collision-induced energy transfer from the $E0_g^+$ state in collision with $I_2(X)$.

$$I_2(E) + I_2(X) \rightarrow I_2(D), \qquad k^{E-D}, \tag{6}$$

$$I_2(D) \rightarrow I_2(X,\text{etc.}) + h\nu, \qquad k_r^D, \tag{7}$$

$$I_2(D) + I_2(X) \rightarrow \text{products}, \quad k_q^D. \tag{8}$$

The decay curve could be fitted with the value $\tau_D(=(k_r^D + k_q^D[I_2])^{-1}) = 10.0 \pm 0.2$ ns. The $D0_u^+$ state lifetime thus obtained is consistent with the collision-free fluorescence lifetime reported for the $D0_u^+$ state ($\tau_D^0 = 13.3$ ns) if we take into account the fast self-quenching rate constant for the $D0_u^+$ state ($\sim 10^{-9}$ cm^3 molecules^{-1} s^{-1}). These results obviously support the conclusion of Fecko *et al.*[17] that spectrum (a) in Fig. 1 arises from the $D0_u^+$ state populated by collision-induced energy transfer from the $E0_g^+$ $v=0$ state. The collision energy transfer rate giving the $D0_u^+$ state, k^{E-D}, cannot be derived by analyzing the time profiles of emissions, so we determined it from the plots of the emission intensity ratios from the $E0_g^+$ and $D0_u^+$ states against the I_2 concentrations.

$$I_{D-X}/I_{E-B} = k^{E-D}[I_2]/k_r^E. \tag{9}$$

Our experiment gives $k^{E-D} = (4.8 \pm 0.6) \times 10^{-11}$ cm^3 molecule^{-1} s^{-1}, which is consistent with the result of Fecko *et al.*[17] It should be pointed out that the $E0_g^+ \rightarrow D0_u^+$ collision energy transfer rate is approximately a factor of 20

smaller than the self-quenching rate constant of the $E0_g^+$ state.

In contrast, the time profiles of fluorescence intensities in Fig. 3 were recorded by using the coaxially aligned pump and probe laser beams. They have completely different features from those shown in Fig. 2. These waveforms are anomalous at several points, indicating that the $D0_u^+$ state is not populated by collision-induced energy transfer from the $E0_g^+$ state but by the $E0_g^+$-$D0_u^+$ transition by ASE.

(1) Waveform (b) observed in $E0_g^+$-$B\ ^3\Pi(0_u^+)$ emission indicates a drastic change in the dynamics in the $E0_g^+$ state. The usual exponential decay of fluorescence signals starts after the probe laser pulse. The fluorescence lifetime estimated from the decay is $\tau \sim 21$ ns, which is consistent with the result from Fig. 2. A small delay can be noticed at the initial rise of the fluorescence signals, which vanishes when the laser intensity is increased. The time profile of the $E0_g^+$-$B\ ^3\Pi(0_u^+)$ emission follows the profile of the probe laser until the middle of the falling edge.

(2) Waveform (c) observed in the $D0_u^+$-$X\ ^1\Sigma_g^+$ emission shows an obvious delay of ~6 ns in the onset of the emission after irradiation by the probe laser pulse. This emission builds up within a few nanoseconds, which is much shorter than the pulse width of the probe laser. The exponential decay starts at the end of falling edge of the probe laser pulse. The estimated lifetime of fluorescence decay is about 11 ns, which agrees with the fluorescence lifetime of the $D0_u^+$ state derived in Fig. 2. However, it is important to note that the apparent decay of the $D0_u^+$ state is much faster than that of the $E0_g^+$ state in this time region. Even though the $D0_u^+$ state is obviously populated through the $E0_g^+$ state, the $E0_g^+ \rightarrow D0_u^+$ conversion is completely removed after the probe laser pulse.

(3) The onsets of the $D0_u^+$-$X\ ^1\Sigma_g^+$ fluorescence signals were found to be unstable against the probe laser pulses, when we examined the signal waveforms on the oscilloscope for every shot. They fluctuated with a time width of a few nanosecond. Furthermore, the shot-to-shot variation of the emission intensity was about a factor of 4, which was several times larger than that of the $E0_g^+$-$B\ ^3\Pi(0_u^+)$ emission observed under the same conditions. This tendency became more apparent when we reduced the probe laser intensity. The $D0_u^+$-$X\ ^1\Sigma_g^+$ emission occurred every several shots, indicating the existence of a threshold in generating the emission.

Furthermore, we observed the ASE signals in the $E0_g^+$-$B\ ^3\Pi(0_u^+)$ transition which was reported by Alekseev *et al.*[18] The time profile of the ASE signals had a sharp spike, whose width (3.1 ns) is much shorter than the duration of the probe laser (6.6 ns) when averaged over 512 shots. The onset of the signals had a shot-to-shot time variation. The width is at least a factor of 2 narrower, which was not apparent from previous experiment.

ASE occurs only between states with an inverted population above a certain threshold determined by factors such as the natural lifetime, the concentration of the excited state, and the length of the media. The inversion population density threshold for ASE is inversely proportional to the square of the stimulated emission wavelength. This suggests that the ASE pulse in the infrared region also occurs in the $E0_g^+$-$D0_u^+$ transition which shares the upper state in common with the $E0_g^+$-$B\ ^3\Pi(0_u^+)$ transition in the ultraviolet. The backward $E0_g^+$-$D0_u^+$ emission exhibited a sharp rise in the fluorescence signals. The generation rate of the $D0_u^+$ state was then derived from its first derivatives, whose temporal behavior was similar to that of the ASE pulse observed in the $E0_g^+$-$B\ ^3\Pi(0_u^+)$ transition. These results imply that the ASE radiative relaxation in the $E0_g^+$-$D0_u^+$ transition populates the $D0_u^+$ state and provides the following $D0_u^+$-$X\ ^1\Sigma_g^+$ emission with a single exponential decay. On the other hand, the ASE relaxation depopulated the $E0_g^+$ state, and the $E0_g^+$-$B\ ^3\Pi(0_u^+)$ emission exhibited a single exponential decay after the ASE pulses. This model is consistent with the results shown in Fig. 3.

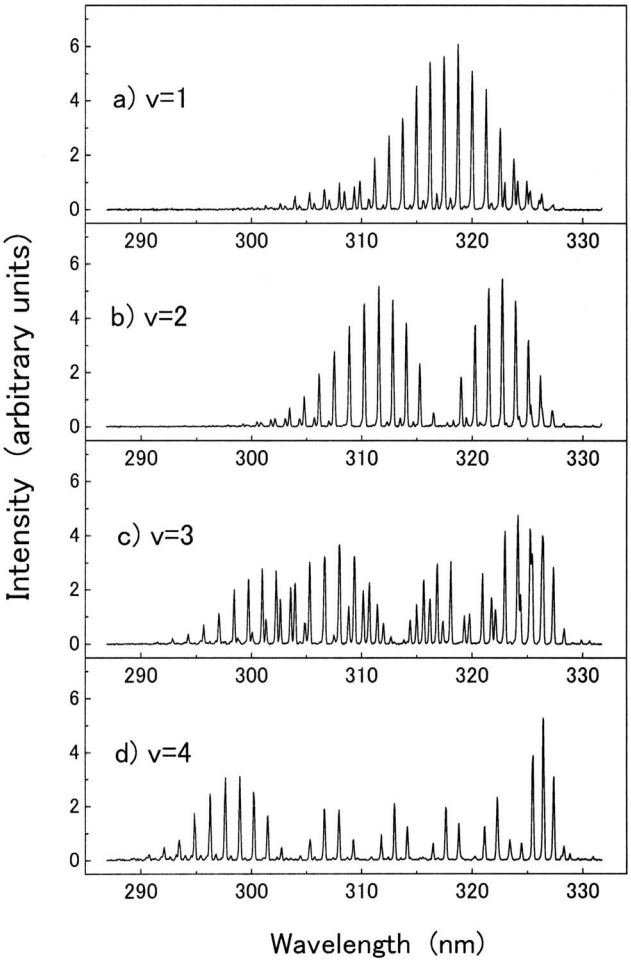

FIG. 5. The $D0_u^+$-$X\ ^1\Sigma_g^+$ emission spectra observed at the excitation to the $E0_g^+$ state in the range of $v=1-4$. The spectral slit width of the monochromator was 0.15 nm. The spectra were recorded by coaxially aligning the pump and probe laser beams. The I_2 sample pressure was 0.173 Torr.

C. $D0_u^+$-$X\ ^1\Sigma_g^+$ emission induced by ASE from the $E0_g^+$ state

Figure 5 shows other examples of the spectra observed from the $D0_u^+$ state that were populated though the ASE pro-

TABLE I. Franck–Condon factors and relative populations of the $D0_u^+$ v'' states observed from the $E0_g^+$ v' state prepared in the range of $v_E=0-4$.

	Initial $E0_g^+$ state									
	$v_E=0$		1		2		3		4	
$D0_u^+$	FCF[a]	P_v[b]	FCF	P_v	FCF	P_v	FCF	P_v	FCF	P_v
$v_D=0$	665	1.00	245	1.00	67.4	⋯	16.7	⋯	4.0	⋯
1	292	0.03	232	⋯	277	1.00	132	⋯	46.7	⋯
2	40.7	0.03	409	0.20	44.8	⋯	214	1.00	165	⋯
3	1.9	⋯[c]	105	⋯	413	0.10	0.0	⋯	127	⋯
4	0.0	⋯	7.6	⋯	179	⋯	352	0.90	25.1	⋯
5			0.1	⋯	18.5	⋯	250	⋯	261	1.00
6					0.4	⋯	35.6	⋯	309	0.05
7							1.0	⋯	59.4	⋯
8									2.2	⋯

[a]FCF$\times 10^3$.
[b]Relative population of the vibrational levels of the $D0_u^+$ state.
[c]Not observed.

cess following the excitation of I_2 to the $E0_g^+$ $v=1-4$ states. The $D0_u^+$-$X\ ^1\Sigma_g^+$ emission is easily saturated by coaxially collimating the two laser beams. In the measurements, the energy flux of the probe laser was large enough to cause saturation. Typically, the outputs of the pump and probe lasers were 1 mJ/pulse. We employed several excitation schemes using different intermediate states to gain access to the $E0_g^+$ $J=55$ state in each vibrational level, and the spectral features were unaffected by the excitation schemes. The spectral resolution of 0.15 nm was insufficient to resolve the rotational structure. However, the vibrational structures were sufficiently well resolved to show the characteristic vibrational distributions in the $D0_u^+$ state in accord with the initially prepared $E0_g^+$ state. Most of the spectra showed emission nearly from a single vibrational level of the $D0_u^+$ state, which can be anticipated from the nodal pattern of the intensity in the envelopes of the vibrational progressions. For example, spectrum (a) contains the dominant emission from a $v=0$ level with a single intensity maximum, spectrum (b) from $v=1$ with double maxima, and so on. Out of these, spectrum (c) is unique, in that it exhibits emissions from two vibrational states with comparable intensities.

In the quantitative analysis of the vibrational distributions in the $D0_u^+$ state, we calculated the Franck–Condon factors between the $D0_u^+$ and $X\ ^1\Sigma_g^+$ states and simulated the spectra from the $D0_u^+$ state in the range $v_D=0-20$ with a spectral resolution corresponding to that of the experiments.[20] They were composed so as to reproduce the spectra. The Franck–Condon factors were relatively insensitive to the breath of the rotational distribution ($\Delta J=\pm 1$ in the $E0_g^+$-$D0_u^+$ transition). In the calculations, we assumed that the rotational angular momentum of the initial $E0_g^+$ state was conserved in the $D0_u^+$ state. Tables I and II summarize the results thus obtained for the vibrational distributions of the

TABLE II. Franck–Condon factors and relative populations of the $D0_u^+$ v'' states observed from the $E0_g^+$ v' state prepared in the range of $v_E=5-9$.

	Initial $E0_g^+$ state									
	$v_E=5$		6		7		8		9	
$D0_u^+$	FCF[a]	P_v[b]	FCF	P_v	FCF	P_v	FCF	P_v	FCF	P_v
$v_D=0$	0.9	⋯[c]	0.2	⋯	0.0	⋯	0.0	⋯	0.0	⋯
1	14.4	⋯	4.1	⋯	1.1	⋯	0.3	⋯	0.0	⋯
2	79.7	⋯	31.1	⋯	10.7	⋯	3.5	⋯	1.1	⋯
3	163	⋯	106	⋯	51.0	⋯	20.9	⋯	7.8	⋯
4	55.6	⋯	136	⋯	118	⋯	70.1	⋯	33.8	⋯
5	72.6	⋯	13.1	⋯	96.1	⋯	116	⋯	84.6	⋯
6	170	⋯	115	⋯	0.0	⋯	55.9	⋯	101	⋯
7	350	1.00	92.8	⋯	139	⋯	9.1	⋯	24.2	⋯
8	89.4	0.05	370	1.00	38.1	⋯	142	⋯	30.3	⋯
9	4.3	⋯	125	0.04	368	1.00	8.0	⋯	127	⋯
10			7.7	⋯	164	0.06	348	1.00	0.0	⋯
11					12.8	⋯	206	0.02	312	1.00
12							20.1	⋯	247	0.02
13									30.0	⋯

[a]FCF$\times 10^3$.
[b]Relative populations of the vibrational levels of the $D0_u^+$ state.
[c]Not observed.

$D0_u^+$ state populated by ASE in the excitation of the $E0_g^+$ state in the range of $0 \leqslant v_E \leqslant 9$. The Franck–Condon factors between the vibrational levels of the $E0_g^+$ and $D0_u^+$ states are also listed for comparison. At vibrational levels higher than these states ($v_E \geqslant 9$), the vibrational distributions of the $D0_u^+$ state were strongly dependent on the laser power. The collision-induced energy transfer reaction might compete with ASE radiative relaxation with an increase in the energy transfer rate; these results are not shown.

The $D0_u^+$ state is populated from the $E0_g^+$ state following the amplification of photons given by spontaneous emission in the $E0_g^+$-$D0_u^+$ system. The gain coefficient G for ASE is given by

$$G = \exp\{(N_{vE} - N_{vD})\sigma_e z\}, \tag{10}$$

where $(N_{vE}-N_{vD})$ is the inversion population between the v_Eth vibrational level of the upper $E0_g^+$ state and the v_Dth vibrational level of the lower $D0_u^+$ state,[21] σ_e is the stimulated emission cross section, and z is the length of the cell. The cross section for stimulated emission is given for the rotational lines in the (v_E, v_D) band of the $E0_g^+$-$D0_u^+$ system,

$$\sigma_e(\nu) = (8\pi^3/3ch)\nu|\mathrm{Re}|^2 q_{vE,vD}(S_{J',J''}/2J'+1)L(\nu), \tag{11}$$

where ν is the transition frequency, $|\mathrm{Re}|^2$ is the transition moment, $q_{vE,vD}$ is the Franck–Condon factor, $L(v)$ is the line shape function, h is Planck's constant, and c is the speed of light. The term $(S_{J',J''}/2J'+1)$ is ~ 0.5 at high J levels.

If we neglect the natural width, the line shape is approximated by the Gaussian function, whose value at the line center is inversely proportional to the transition frequency ν. The gain coefficient at the line center is then only dependent on the Franck–Condon factor for a given (v_E, v_D) transition, suggesting that the $D0_u^+$ v'' state populated by ASE has the largest Franck–Condon factor with the $E0_g^+$, v' state initially prepared. As the calculated Franck–Condon factors for the $E0_g^+$-$D0_u^+$ transition are shown, our observations are consistent with this prediction in the excitation to the $E0_g^+$ state at the $v_E=0$ level, as shown in Table I, and at the $5 \leqslant v_E \leqslant 9$ levels, as shown in Table II. However, it fails to account for the results at the excitation to the $E0_g^+$ state in the range of $1 \leqslant v_E \leqslant 4$ given in Table I. The spectra show the emission originating from the vibrational state with the second-largest Franck–Condon factor.

These phenomena might be produced by two related reasons. First, the ion-pair states have transitions that terminate on the valence states in the ultraviolet region, some of which have extremely large transition moments. These transitions make their natural lifetimes relatively short. Furthermore, the lifetimes of the excited states are shortened by collisions with $I_2(X)$, as demonstrated by the $E0_g^+$ $v=0$ state in this experiment. The fluorescence lifetimes of the $E0_g^+$ and $D0_u^+$ states under the experimental conditions are 20.9 and 10.0 ns, respectively, as shown in Fig. 2, which denote a homogenous linewidth of 7.84×10^{-4} cm^{-1} for the $E0_g^+$-$D0_u^+$ transition in terms of the uncertainty principle. On the other hand, the Doppler widths at room temperature are several tenths of the homogeneous linewidth in the energy region where the vibrational bands of the $E0_g^+$-$D0_u^+$ transition are expected. Under these conditions, the cross sections for stimulated emission at the line center are no longer independent of the transition frequencies.

For example, in the excitation of the $E0_g^+$ $v_E=1$ state, we observed strong emission bands from the $D0_u^+$ $v_D=0$ state, together with much weaker bands from the $v_D=2$ state. The radiative relaxation by ASE dominantly occurs at 487 cm^{-1} in the $v_E=1 \rightarrow v_D=0$ transition, whose Franck–Condon factor is 0.245. However, the initially prepared $v_E=1$ state has the largest Franck–Condon factor of 0.409 with the $v_D=2$ state, whose transition occurs at 298 cm^{-1}. The Doppler width is 3.78×10^{-4} cm^{-1} in the transition at 487 cm^{-1} and 2.31×10^{-4} cm^{-1} at 298 cm^{-1}. Assuming a homogeneous linewidth of 7.84×10^{-4} cm^{-1}, the ratio of cross sections for stimulated emission from $v_E=1$ is derived to be 0.91 for the $v_D=0/v_D=2$ pair of levels, which is obviously larger than the corresponding ratio of 0.60 calculated from the Franck–Condon factors. The ratio of cross sections for the $v_D=1/v_D=3$ pair of levels in the transitions from $v_E=2$ is 1.00, $v_D=2/v_D=4$ from $v_E=3$ is 0.91, and $v_D=5/v_D=6$ from $v_E=4$ is 1.16. On the other hand, the ratio of Franck–Condon factors is 0.67 for the $v_D=1/v_D=3$ pair of levels, 0.61 for $v_D=2/v_D=4$, and 0.84 for $v_D=5/v_D=6$.

These estimations of the ASE transition probabilities include the effect of homogeneous broadening by inelastic collisions, so-called quenching collisions, which are apparent in our experiment. In addition, elastic collisions are known to cause the spectral line shift arising from the interaction between the collision pair, which provides another mechanism for spectral broadening. Since a strong interaction between $I_2(E0_g^+)$ and $I_2(X)$ was demonstrated,[16] this effect might cause the ASE transition probability in the higher frequency band to be much closer to that in the lower one, or even larger in some cases, in spite of its small Franck–Condon factor.

Second, the photon flux initially seeded for stimulated emission is derived from the usual formula for the band intensities in emission,

$$\rho^{v',v''} = (64/3c^3h)\pi^4 N_v \nu^3 |\mathrm{Re}|^2 q_{v',v''}. \tag{12}$$

With an increase in the transition frequency, we can expect an increase in the number of photons seeded for ASE. These effects promote ASE relaxation in the vibrational band at higher frequencies, and cause the $D0_u^+$ populations to deviate from the relevant Franck–Condon factor.

D. Comparison with other studies

The most striking feature of this experiment is that it demonstrates that electronic relaxation occurs in the $E0_g^+$-$D0_u^+$ transition by ASE, and that this occurs without collisions. It produces the anomalous intense emission of the $D0_u^+$-$X\ ^1\Sigma_g^+$ system observed by Fecko *et al.*[17] They reported that the $D0_u^+$-$X\ ^1\Sigma_g^+$ emission signal increased 75-fold with a fourfold increase in the pressure from 40 to 160 mTorr at the excitation of $v_E=0$, even though the process was unsettled. On the other hand, Inard *et al.*[13] reported the fluorescence spectrum from the $D0_u^+$ state when the $E0_g^+$ $v=1$ state was initially prepared. They used two dye lasers with continuous

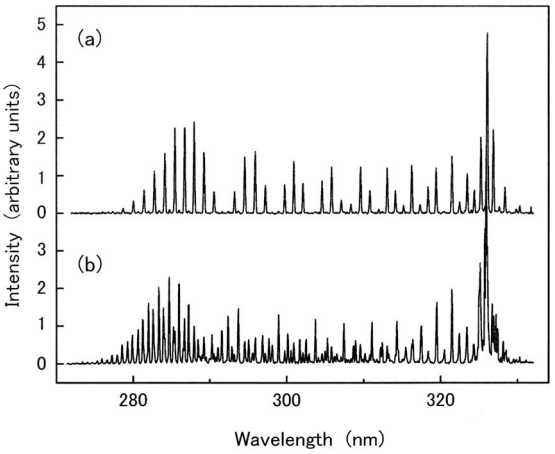

FIG. 6. The $D0_u^+$-$X\ ^1\Sigma_g^+$ emission spectra observed at the excitation to the $E0_g^+$ $v=8$ state following (a) the $E\rightarrow D$ radiative relaxation by ASE and (b) the $E\rightarrow D$ energy transfer by collisions. The spectral slit width of the monochromator was 0.15 nm. The I_2 sample pressure was 0.173 Torr.

operation, but unlike other studies, they did not use pulsed lasers. The vibrational levels of the $D0_u^+$ state were then populated in the ratios of $N_4/N_3/N_2=0.33:1.00:0.11$, where N_i is the population ratio of the i-th vibrational level of the $D0_u^+$ state. These population ratios do not agree with those shown in spectrum (a) of Fig. 5, which we observed at the excitation to the $v_E=1$ state. The $v_D=0$ level is favored to be populated from $v_E=1$. It should be noted that our result on the $D0_u^+$-$X\ ^1\Sigma_g^+$ emission spectrum arising from the collision-induced relaxation indicates the population ratios $N_5/N_4/N_3/N_2/N_1=0.4:0.2:1.0:0.1:0.1$ in the $D0_u^+$ state at the $v_E=1$ excitation, which appear to be consistent with the observations of Inard *et al.*[13] They used cw laser excitation to prepare the $E0_g^+$ $v=1$ state, whose population did not exceed the threshold for ASE.

In the excitation of the $E0_g^+$ state at higher vibrational levels, two groups reported different vibrational distributions of the $D0_u^+$ state resulting from the collision-induced energy transfer. The largest discrepancy was found in their data on the relative population of the $D0_u^+$ state formed after optical excitation of $v_E=8$ level. The population ratio was reported to be $N_{12}/N_{11}/N_{10}=0.08:0.15:1.00$ by Ubachs *et al.*[11] and $N_{12}/N_{11}/N_{10}=0.24:0.24:1.00$ by Teule *et al.*[12] On the other hand, Bibinov *et al.*[15] reported the vibrational distribution from the $E0_g^+$ $v=8$ and $J=55$ state, with $N_{12}/N_{11}/N_{10}=0.28:1.00:0.26$, showing a marked difference in the most populated vibrational state.

As our result shown in spectrum (a) of Fig. 6 shows, the ASE process from the $E0_g^+$ $v=8$ state results in the $D0_u^+$ $v=10$ state being predominantly populated with the population ratios $N_{12}/N_{11}/N_{10}=0.00:0.02:1.00$. This distribution is similar to the previous results reported by Ubachs *et al.*[11] and by Teule *et al.*[12] On the other hand, collision-induced energy transfer gives spectrum (b), indicating the population ratios $N_{12}/N_{11}/N_{10}/N_9/N_8=0.61:1.00:0.42:0.01:0.01$, which is close to the results of Bibinov *et al.*[15] It is likely that the ASE process contributes to populating the $D0_u^+$ state in addition to the collision-induced energy transfer observed in the experiments of Ubachs *et al.*[11] A coaxial alignment of laser beams was used in the experiments of Ubachs *et al.*[11] and Teule *et al.*,[12] as described in their papers. In our experiments, ASE easily occurred for the $E0_g^+$-$D0_u^+$ transition even at an I_2 pressure of less than 100 mTorr, when two pulse laser beams with ~1 mJ outputs were coaxially introduced into a 10 cm cell.

Finally, it should be pointed out that the $D0_u^+$-$X\ ^1\Sigma_g^+$ emission spectra observed in our experiment differ from those reported in the excitation of $v_E=1$ and 2 by Alekseev *et al.*[18] Their spectra showed that the $D0_u^+$ state was predominantly populated at $v_D=2$ and 3 in the excitation of $v_E=1$ and 2, respectively, and that the Franck–Condon factors between the $E0_g^+$ and $D0_u^+$ states dominated the $E0_g^+\rightarrow D0_u^+$ population transfer by ASE.

Alekseev *et al.*[18] performed double-resonance excitation of I_2 using a different experimental configurations from ours. They used counterpropagating pump and probe laser beams that were temporally overlapped. They also used different cell length and pulse duration of the excitation lasers. In connecting these factors, they succeeded to select conditions that are suitable for promoting the ASE radiative relaxation through the vibrational band having the largest Franck–Condon factor.

In our experimental arrangements, the tests were carried out to reproduce the emission spectra reported by Alekseev *et al.*[18] We introduced the pump and probe lasers coaxially into the 10 cm long cell from the same direction. The windows were adjusted so that the reflected light propagated along the optical path of the incident beams. We usually observed the emission spectra through the side window in the center of cell. The emission intensity showed a strong dependence on the excitation laser beam. In particular, the intensity observed in the vicinity of the front widow was about an order of magnitude stronger than that at the rear window.

Under the conditions, from the $E0_g^+$ $v=1$ level, spectrum (a) in Fig. 1 reported by Alekseev *et al.*[18] was recorded in the vicinity of the rear window by reducing the beam diameter of the probe laser to 1 mm by using an aperture. In this case, the emission intensity and profile were quite sensitive to the angle of the sample cell relative to the incident beams and also to the beam diameter of the probe laser beam. By varying the cell angle by several degrees, we lost the strong emission originating from the $D0_u^+$ $v=2$ state which has the largest Franck–Condon overlap with the laser excited level of the $E0_g^+$ $v=1$ state. Furthermore, by returning the diameter of the probe laser beam to 3 mm, we observed an increase in emission intensities of more than an order of magnitude, and the spectral features were drastically changed to show the emission from the $D0_u^+$ $v=0$ state, as shown in spectrum (a) of Fig. 5. These findings indicate that these two infrared transitions compete in the $E0_g^+\rightarrow D0_u^+$ radiative relaxation by ASE, and their occurrences strongly depend on the experimental configuration.

The $E0_g^+$ $v=1\rightarrow D0_u^+$ $v=2$ transition is favored to occur under the condition that the photon flux can travel back and forth along the amplifying media. The backreflected light from the windows is then important to increase the total amplification, and the population of the $v_D=2$ state prevails

over that of the $v_D=0$ state in terms of the advantage of the large cross section at the center line. On the other hand, enlarging the probe laser beam diameter increases the number of photons seeded for ASE and the gain active volume, which increases the emission intensity. However, the fraction of ASE output escaping from the gain volume may increase after reflection at the windows. This reduces the average gain coefficient, and the radiative relaxation to the $v_D=0$ state can be promoted due to the increase in the number of photons seeded for ASE.

[1] R. S. Muliken, J. Chem. Phys. **55**, 288 (1971).
[2] K. P. Huber and G. Herzberg, *Molecular Spectra and Structures. IV. Constants of Diatomic Molecules* (Van Nostrand-Reinhold, New York, 1979).
[3] J. C. D. Brand and A. R. Hoy, Appl. Spectrosc. Rev. **23**, 285 (1987).
[4] Y. Nakano, H. Ukeguchi, and T. Ishiwata, J. Chem. Phys. **121**, 1397 (2004).
[5] S. Motohiro, S. Nakajima, K. Aoyama, E. Kagi, and T. Ishiwata, J. Chem. Phys. **117**, 9777 (2002).
[6] G. W. King, I. M. Lottlewood, and J. R. Robins, Chem. Phys. **56**, 145 (1981).
[7] J. C. B. Brand, A. R. Hoy, and D. C. P. Tse, Can. J. Spectrosc. **30**, 43 (1985).
[8] T. Ishiwata and I. Tanaka, Laser Chem. **7**, 79 (1978).
[9] T. Ishiwata, T. Yotsumoto, and S. Motohiro, Bull. Chem. Soc. Jpn. **74**, 1605 (2001).
[10] S. Motohiro, S. Nakajima, and T. Ishiwata, J. Mol. Spectrosc. **212**, 194 (2002).
[11] W. Ubachs, I. Aben, J. B. Mila, G. J. Somsen, A. G. Stuiver, and W. Hogervorst, Chem. Phys. **174**, 285 (1993).
[12] R. Teule, S. Stolte, and W. Ubachs, Laser Chem. **18**, 111–128 (1999).
[13] D. Inard, D. Cerny, M. Nota, R. Basic, S. Churassy, and V. Skorokhodov, Chem. Phys. **243**, 305 (1999).
[14] M. E. Akopyan, N. K. Bibinov, D. B. Kokh, A. M. Pravilov, M. B. Stepanov, and O. S. Vasyutinskii, Chem. Phys. **242**, 263 (1999).
[15] N. K. Bibinov, O. L. Malinina, A. M. Ptavilov, M. B. Stepanov, and A. A. Zakharova, Chem. Phys. **277**, 179 (2002).
[16] T. Tscherbul, A. A. Buchachenko, M. E. Akopyan, S. A. Porestsky, A. M. Pravilov, and T. A. Stephenson, Phys. Chem. Chem. Phys. **6**, 3201 (2004).
[17] C. J. Fecko, M. A. Freedman, and T. A. Stephenson, J. Chem. Phys. **115**, 4132 (2001).
[18] V. A. Alekseev, T. Ridley, K. P. Lawley, and R. J. Donovan, Chem. Phys. Lett. **443**, 34 (2007).
[19] T. Ridley, K. P. Lawley, R. J. Donovan, and V. Alekseev, Phys. Chem. Chem. Phys. **9**, 5885 (2007).
[20] R. J. LeRoy, "RKR1: A Computer Program Implementing the First-Order RKR Method for Determining Diatomic Potential Energy Curves from Spectroscopic Constants," University of Waterloo Chemical Physics Research, Report CP-425, 1992.
[21] Y.-L. Huang and R. J. Gordon, J. Chem. Phys. **97**, 6363 (1992).